Enhanced treatment of perfluoroalkyl acids in groundwater by membrane separation and electrochemical oxidation

Alvaro Soriano [a], Charles Schaefer [b], Ane Urtiaga [a,*]

[a] Department of Chemical and Biomolecular Engineering, University of Cantabria, Av. Los Castros s/n, 39005 Santander, Spain
[b] CDM Smith, 110 Fieldcrest Avenue, Edison 08837, NJ, USA

ABSTRACT

This work explores the treatment of poly- and perfluoroalkyl acids (PFAAs) in groundwater by coupling membrane separation and electrochemical oxidation (ELOX). A process system engineering approach based on modelling and empirical data was followed. Two nanofiltration (NF90) and reverse osmosis (BW30) membranes were characterized for treating an electrolyte (NaCl and CaSO$_4$) mixture of perfluorocarboxylic acids (PFCAs) containing PFOA, PFHpA, PFHxA, PFPeA and PFBA with initial concentrations of 10 µg L^{-1} each. Membrane surface charge shielding and concentration polarization negatively influenced NF90 performance, and the BW30 membrane was selected. Electrochemical oxidation with boron doped diamond anodes treated the PFCAs mixture amended with PFOS and 6:2 FTSA, emulating previously pre-concentrated feed and non-preconcentrated feed conditions. Working at different current densities (J) between 20 and 350 A m^{-2}, the removal of PFOA, PFOS and 6:2 FTSA followed first order apparent kinetics, although shorter chain PFCAs initially showed increasing trends because of their simultaneous electrogeneration and degradation. Overall, ΣPFAA electrolysis followed first order kinetics linearly correlated to J in the full range of testing. Unexpectedly, PFAAs electrolysis was faster for the low conductive non-preconcentrated feed, a result that was ascribed to the enhanced direct electron transfer mechanism resulting from the higher cell voltage. For 99.9% PFAAs removal, the total specific cost of treatment was minimized using a cascade of four RO stages and ELOX treatment of the concentrate, to reach ΣPFAA below the Health Advisory Levels recommended by the USEPA in drinking water (<70 ng L^{-1} sum of PFOA and PFOS).

1. Introduction

Poly- and perfluoroalkyl acids (PFAAs) are a class of highly persistent chemicals that are extremely resistant to chemical, physical and biological degradation [1]. Indeed, PFAAs are highly mobile and their occurrence has been extensively reported around the globe, in rivers and human drinking water resources [2,3], in soils [4], in landfills [5], in wastewater treatment plants (WWTP) [6] or groundwater impacted by aqueous film-forming foam (AFFF) [7]. Overall, it is considered that the use of AFFF is an important local source of PFAAs contamination in soil and water bodies [8], either due to the direct presence of PFAAs in the AFFF formulations, or by transformation of fluorinated compounds in the AFFF that are subject to abiotic or biotic transformations that form the more recalcitrant PFAAs [9–11]. Contamination of water bodies (e.g., surface water, groundwater) by AFFF has been associated with fire-training sites located in military bases [12,13] and airports [14], or as a result of the extinction of catastrophic fires.

Conventional wastewater treatment methods have proven to be ineffective to remove PFAAs from impacted water bodies [15]. There-fore, recent research efforts have been directed towards the development of innovative removal and destruction technologies for the treatment of these substances. Granular activated carbon (GAC), powder activated carbon (PAC) and anion exchange resins [16–19] are the most extensively studied adsorbents for PFAA removal from water. However, adsorption techniques have several disadvantages, such as the decline of the sorption efficiency for short-chain PFAAs [20], their low regeneration efficiency, and when applicable, the generation of large amounts of waste organic solvents used as regenerants [21]. Alternative attempts to regenerate anion exchange resins rely on the use of cosolvents, which provides additional complexity to the overall treatment process [17,22,23]. Alternatively, the adsorption media must be incinerated at high temperatures (>1000 °C) [24].

Other approach for separating PFAA from impacted waters is to apply pressure-driven membrane processes (mainly nanofiltration (NF) and reverse osmosis (RO)) to effectively retain PFAAs. While RO generally achieves higher PFAAs rejections than NF, its water filtration productivity is considerably lower [25,26]. Nevertheless, a disadvantage of membrane processes is that the PFAAs retained in the concentrate typically require further treatment.

The electrochemical oxidation (ELOX) of PFAAs has shown very promising results. Specifically, the use of ELOX by means of boron doped diamond (BDD) anodes can satisfactorily mineralize PFAAs, as well as PFAAs precursors, to CO_2 and fluoride anions [27–30]. However, widescale application of ELOX for treatment of PFAA-impacted waters remains challenging due to the associated high energy consumption [31] and the high capital costs of BDD electrochemical cells [32]. Also, these compounds are usually present at very low concentrations in groundwater impacted by AFFF [13], which exacerbate mass transfer kinetic limitations. To mitigate these mass transfer limitations at low PFAA concentrations, membrane separation can be used as a pre-concentration stage to increase PFAAs levels in the retained water prior to ELOX treatment. This will facilitate implementation of ELOX at a lower overall cost compared to that of electrochemical degradation alone [33]. Although this approach has been recently tested for the treatment of industrial process waters which contained perfluorohexanoic acid in the concentration range of hundreds of mg L^{-1} [34,35], assessment of this approach using a mixture of PFAAs in the μg L^{-1} range [36] and in the presence of a common fluorotelomer PFAAs precursor (6:2 fluorotelomer sulfonic acid (6:2 FTSA)) [37] would provide improved insight into the efficacy of this approach for remediation of groundwater impacted by AFFF.

In this work, we explore the integration of pressure-driven membrane processes with electrochemical oxidation for the treatment of PFAAs in concentrations relevant to AFFF-impacted groundwater. Initial testing focused on NF and RO treatment of a perfluorinated carboxylic acid (PFCA) mixture, followed by ELOX of the PFCA concentrate (amended with perfluorooctane sulfonic acid (PFOS) and 6:2 FTSA) using BDD anodes, at several current densities. The empirical information obtained in these experiments was implemented in an optimization model with the objective of minimizing the total costs of the integrated process, considering capital and operating costs. New insights on the favourable impact of increasing the current density on the reduction of the total costs of the integrated process were also evaluated.

2. Materials and methods

2.1. Materials

Two thin-film composite polyamide nanofiltration (NF90) and reverse osmosis (BW30) membranes, purchased from Dow FilmTec, were tested in the filtration experiments. The NF90 is a tight nanofiltration membrane for production of drinking water and demineralization applications, which is characterized by its medium to high productivity (the membrane permeability L_p ranges from 5.8 to 10.4 L m^{-2} h^{-1} bar^{-1} depending of the feed water and operating conditions [38]), while the BW30 membrane is commercialized for brackish water desalination applications, with lower water fluxes (L_p in the range 3.8 – 4.6 L m^{-2} h^{-1} bar^{-1}) [38,39]. Expected PFAAs rejections are typically higher than 90%, although most previous studies were performed at much higher PFAA concentrations [38,40], or reported estimated rejections [41]. PFAAs used to spike aqueous solutions were the following: perfluorobutanoic acid (PFBA) (≥99%), perfluoropentanoic acid (PFPeA) (97%), perfluorohexanoic acid (PFHxA) (≥97%), perfluoroheptanoic acid (99%), perfluorooctanoic acid (PFOA) (95%) and PFOS potassium salt (≥98%), all purchased from Sigma-Aldrich. 6:2 FTSA, which was used to spike aqueous solutions, was supplied by Synquest laboratories. Calcium sulfate dihydrate (≥ 98%) and UHPLC-MS grade methanol (≥ 99.9%) were purchased from Scharlau. Sodium chloride (≥99%) was supplied by Panreac. A Milli-Q® Advantage A10 Water Purification System (Millipore) produced ultrapure water for preparing the aqueous solutions.

For the NF/RO experiments, ultrapure water was spiked to obtain 10 μg L^{-1} of each target PFCA and electrolyte (100 mg L^{-1} NaCl and 100 mg L^{-1} CaSO$_4$). Ions such as sodium, calcium, sulfate and chloride, can be typically found dissolved in AFFF impacted groundwater

[13,42]. The pH of the resulting solution was 6.3. The PFCA concentrations targeted in the aqueous solutions were prepared based on the concentrations observed in AFFF-impacted groundwater [42,43]. Literature information about the characteristics of AFFF-impacted groundwater can be found in Table S1 of supplementary material. It is recognized that many of the polyfluorinated PFAA precursors that are often found in AFFF-impacted source area waters were not included in this current study, as the focus was on the more recalcitrant PFAAs [30].

For the electrolysis experiments, the feed solution was prepared with PFOA, PFHpA, PFHxA, PFPeA and PFBA, 6:2 FTSA and PFOS. 6:2 FTSA and PFOS were included in the ELOX testing, although they were not considered initially in the filtration experiments, to provide insight into the electrochemical treatment of perfluorinated sulfonates and a common fluorotelomer PFCA precursor. Electrolysis experiments were initially performed with the PFAAs mixture without preconcentration, where the initial concentration of individual PFAA was 10 μgL^{-1} and Na$_2$SO$_4$ (0.21 g L^{-1}) was used as electrolyte. Compared to filtration tests, in electrolysis experiments sodium sulfate replaced chloride and calcium salts, to assure the long-term stability of the electrolyte solution. Otherwise, chloride would evolve to chlorine, and eventually to perchlorate at elevated applied current densities. Na$_2$SO$_4$ (0.21 g L^{-1}) was calculated to have similar equivalent saline concentration ($C_{eq} = 0.5 \sum_{i=1}^{s} |z_i| C_{F,i}|$, being z the ionic valence [44]) to the NF/RO feed solution. Next, electrolysis was performed considering a volume reduction factor $VRF = 10$ (VRF is the ratio between the initial feed volume and the final time feed volume), a situation equivalent to a ten times reduction of the initial feed volume, that is accompanied by a significant increase of PFAS and electrolyte concentration in the retentate. Thus, in electrolysis experiments the initial concentration of each PFAA compound in the feed mixture varied from 35 to 220 μg L^{-1}, and the concentration of Na$_2$SO$_4$ used as supporting electrolyte was 1.5 L^{-1}, that is equivalent to the saline concentration obtained in the NF concentrate.

2.2. Filtration experiments

Filtrations experiments were carried out using a laboratory scale rectangular cross-flow test cell (SEPA-CF, GE Osmonics), with an effective membrane area 155 cm^2, channel height 1.7 mm and channel width 9.5 cm. An illustration of the experimental set-up is shown in Figure S1 of the supplementary material. Flat-sheet membrane coupons were soaked in ultrapure water for 24 h and then housed in the membrane cell. The cross-flow velocity of the feed stream inside the membrane cell was 24.7 cm s^{-1}. More experimental details can be found elsewhere [38]. After membrane compaction, 10 L of fresh feed solution were introduced into the feed tank. The operating pressure was fixed at 10 bar in the feed chamber of the membrane test cell. As membrane filtration experiments were aimed to concentrate PFAAs in the aqueous solution, only the retentate stream was recycled to the feed tank, while the permeate volume was collected in a separated tank. The pre-concentration phase was terminated when a VRF of 10 was obtained. All permeate and feed samples were collected in polypropylene certified vials and stored at 4 °C until analysis.

2.3. Electrochemical oxidation experiments

Batch ELOX experiments were performed using the experimental set-up depicted in Figure S1 of the supplementary material. The electrochemical cell (DiaCell 201 PP, Adamant Technologies) consisted of two parallel flow-by compartments made of a circular central bipolar p-Si/BDD electrode. Each anode had a surface area of 70 cm^2, resulting in a total anodic area of 140 cm^2. The cathodes also consisted of p-Si/BDD, with the same area as the anodes. Each compartment worked in an undivided mode, with an interelectrode gap of 1 mm. The electrochemical cell was connected to a power supply (Vitecom 75-HY3005D). The feed solution was maintained at 20 °C. Experiments were performed under
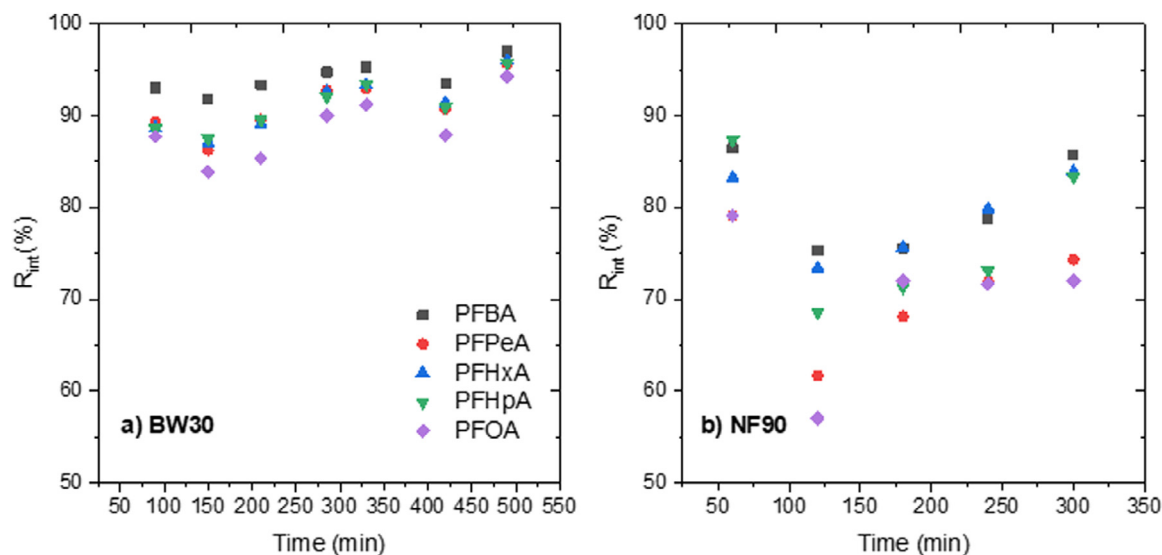
Fig. 1. PFCA observed rejection (R_{obs}) evolution with time using the BW30 and the NF90 membranes, in concentration mode experiments. $C_{0,each\ PFCA} = 10\ \mu g\ L^{-1}$. $C_{0,electrolyte} = 100\ mg\ L^{-1}\ NaCl + 100\ mg\ L^{-1}\ CaSO_4$. Feed $P = 10\ bar$.

galvanostatic conditions. Samples were collected in polypropylene certified vials and stored at 4 °C until analysis.

2.4. Analytical methods

PFAA concentrations in all samples were quantified using a liquid chromatography system (Acquity H-Class, Waters) coupled to a triple-quadrupole mass spectrometer (Acquity TQD, Waters) with an electrospray ionization (ESI) interface operated in the negative ionisation mode. The column used for the analytical separation was the Waters UPLC BEH C18 (1.7 μm, 2.1 × 50 mm), thermostated at 50 °C. The eluents were (i) an ammonium acetate 2 mmol L^{-1} and 5% of methanol aqueous solution (A) and (ii) pure methanol (B). The flow rate of the mobile phases was 0.4 mL min^{-1} in gradient mode. Values of LOQ for every PFAA are the following: PFBA (0.14 μg L^{-1}), PFPeA (0.44 μg L^{-1}), PFHxA (0.38 μg L^{-1}), PFHpA (0.43 μg L^{-1}), PFOA (0.04 μg L^{-1}), PFOS (0.44 μg L^{-1}), 6:2 FTSA (0.70 μg L^{-1}). LOQs were estimated as the lowest concentration of each PFAA compound in the matrix sample giving a peak area equal to the blank signal plus ten times the standard deviation of the blank [45].

3. Results and discussion

3.1. PFCAs pre-concentration by NF and RO

Fig. 1 shows significant differences in PFCAs rejection between the two membranes considered in this study. Individual PFCA concentrations in feed and permeate sides used for rejections calculation are given in Figure S2 of the supplementary material. Using the BW30 membrane, PFCA rejection ranged from 84% to 95.9% (observed rejections are reported). The NF90 membrane provided lower rejections compared to the BW30 membrane, as maximum rejection in the NF90 membrane reached 88%. The attained observed rejection values are lower than those reported in our previous work where we evaluated several NF and RO membranes in the separation of PFHxA at comparatively elevated concentrations of 100 mg L^{-1}, which were relevant in industrial process streams [38]. One plausible explanation for the reduced NF performance in this study is the presence of divalent calcium cations. Ca^{2+} cations are highly rejected during NF filtration and may introduce charge-shielding effects, thus severely decreasing the electrostatic repulsion between the negatively charged perfluorcarboxylates in the feed solution and the membrane surface, which is negatively charged at the circumneutral

operating pH, as reported in previous studies [46]. It is noted that observed rejections values are influenced by concentration polarization at the boundary layers, with the effect of reducing the observed rejection at increasing permeate fluxes, as occurs in the NF90 membrane compared to the BW30 RO membrane. The effect of concentration polarization is more pronounced at very low PFCA concentrations. To prove the negative effect of concentration polarization, intrinsic membrane rejections ($R_{intrinsic}$) were calculated and are provided in Figure S3 of supplementary material. The BW30 membrane maintained PFCAs intrinsic membrane rejections over 95%, while in the case of the NF90 membrane, the intrinsic membrane rejections were mostly over 90%. Notably, calculated intrinsic rejection values are much closer than observed rejections among the PFCA compounds under study. Overall, we attribute the unexpected low rejections observed with the NF90 membranes to the combined effect of its higher water flux that increased the PFCA concentration gradient across the membrane as a result of concentration polarization phenomena, and the presence of calcium cations that reduced the electrostatic repulsion of negatively charged perfluorocarboxylates.

For design purposes, and for parameterization of the filtration-ELOX model [34], we selected the BW30 membrane to carry out the optimization study, since the PFCAs rejection by the NF90 membrane was poorer when dealing with the simulated AFFF impacted groundwater matrix. Fig. 2 shows the PFCAs concentrations in the permeate (C_p) as a function of the PFCAs concentrations in the retentate (C_F) for the BW30 membrane. PFCAs concentrations were varying as a function of time (Figure S2 of supplementary material) as a result of the filtration experiments being performed in concentration mode. The data in Fig. 2 were reasonably described by a linear correlation, which facilitates its functionality into the optimization study. The BW30 hydraulic permeability, in these experiments, was $L_{p,\ BW30} = 5.1 \pm 0.7\ L\ m^{-2}\ h^{-1}\ bar^{-1}$.

3.2. Electrochemical oxidation of PFAAs

Fig. 3 presents the evolution with time of individual PFAAs during the electrochemical degradation experiments, at three values of the applied current density (20, 50 and 350 A m^{-2}) and two *VRF* conditions: i) *VRF*=1, which corresponds to the situation in which no NF/RO preconcentration is carried out, and ii) *VRF*=10, in which the initial feed volume was reduced ten times by RO preconcentration, at the same time the concentrations of PFAAs and salts was increased. In all cases, Fig. 3 shows that the concentrations of PFOA, PFOS and 6:2 FTSA, which
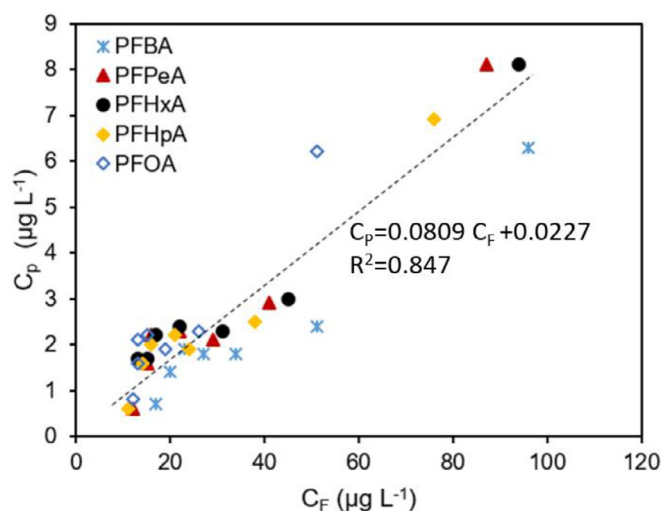
Fig. 2. BW30 membrane. PFCA concentration in the permeate vs. PFCA concentration in the feed tank, in concentration mode experiments. Feed P = 10 bar.

Table 1
Kinetic constants of PFOA, PFOS and 6:2 FTSA BDD electrolysis, obtained from the fitting of experimental data in Fig. 4 to first order rate kinetics. Apparent (k'_{app}) and electrode area/volume treated normalized (k').

J (A m^{-2})	VRF = 1		VRF = 10	
	k'_{app} (min^{-1})	k' (m min^{-1})	k'_{app} (min^{-1})	k' (m min^{-1})
PFOA 20	0.023	0.0017	0.022	0.0016
50	0.063	0.0045	0.045	0.0032
350	0.23	0.017	0.099	0.0071
PFOS 20	0.014	0.0010	0.0046	0.00033
50	0.027	0.0019	0.0098	0.0007
350	0.14	0.0098	0.043	0.0031
6:2 20	0.046	0.0033	0.035	0.0025
FTSA 50	0.094	0.0067	0.048	0.0034
350	0.17	0.012	0.081	0.0058

L A^{-1} min^{-1}) are defined as follows,

$$k' = \frac{k'_{app}V}{A_e} \tag{1}$$

$$k'_n = \frac{k'_{app}V 10^3}{J A_e} \tag{2}$$

where k'_{app} is the apparent kinetic constant (min^{-1}) that was obtained from the fitting of concentration data of individual compounds vs. time to a first order kinetic model, V is the electrolyzed volume (m^3), A_e is the electrode area (m^2) and J is the applied current density (A m^{-2}). Table 1 shows k'_{app} and k' values for long-chain PFOA, PFOS and 6:2 FTSA in all the VRF and J conditions studied. Previous results related to the BDD oxidation of 6:2 FTSA [29] at 50 A m^{-2} (k' = 0.0026 m min^{-1}), PFOA [50] at 50 A m^{-2} (k' = 0.005 m min^{-1}) and PFOS [43] at 150 A m^{-2} (k' = 0.0027 m min^{-1}) are in good agreement with the results of this study, some rate constants being slightly higher than the previously reported values. In general, PFOS was found to experience the slowest degradation at any current density, with measured rate constants being roughly one half to one fourth of the observed rates for PFOA and 6:2 FTSA at comparable conditions; Schaefer et al. [43] and Zhuo et al. [47] also showed that PFOS was less reactive than PFOA during electrochemical treatment using BDD anodes.

Fig. 4 presents the evolution of the sum concentration of all PFAAs (ΣPFAA). Noticeably, the evolution with time of ΣPFAA fits first-order apparent kinetics, at any current density. Both the increase of the applied current density and the increase of the cell potential at low VRF conditions had a positive effect on the ΣPFAA degradation kinetics.

The linear fitting of the first order kinetic constant after correction with the volume and anode area, k', as a function of the applied current density (Fig. 4b), was used in the optimization model, as described in the following section. For additional comparison with different electrochemical oxidation systems, the current-normalized first order kinetic constants (k'_n) of ΣPFAA has been also calculated as follows: at VRF = 1, 8.6×10^{-4} L A^{-1} min^{-1} (at J = 20 A m^{-2}), 2.2×10^{-3} L A^{-1} min^{-1} (at J = 50 A m^{-2}), and 6.3×10^{-3} L A^{-1} min^{-1} (at J = 350 A m^{-2}); at VRF=10, 1.7×10^{-4} L A^{-1} min^{-1} (at J = 20 A m^{-2}), 1.5×10^{-4} L A^{-1} min^{-1} (at J = 50 A m^{-2}), and 1.6×10^{-4} L A^{-1} min^{-1} (at J = 350 A m^{-2}). From these values it can be seen that, at VRF=1 conditions, the current efficiency of the anodic oxidation increases as the applied current density increases, while, on the contrary, at VRF=10 the increase of the applied current density does not vary the current efficiency of the process. As was discussed previously, this may be related to promoted fast DET reactions at the surface of the BDD electrode at high cell potentials.

3.3. Integration of preconcentration and electrooxidation for treatment of PFAAs impacted simulated groundwater

Fig. 5 illustrates the proposed integration of membrane preconcentration and electrochemical degradation. Fig. 5 also includes the opti-
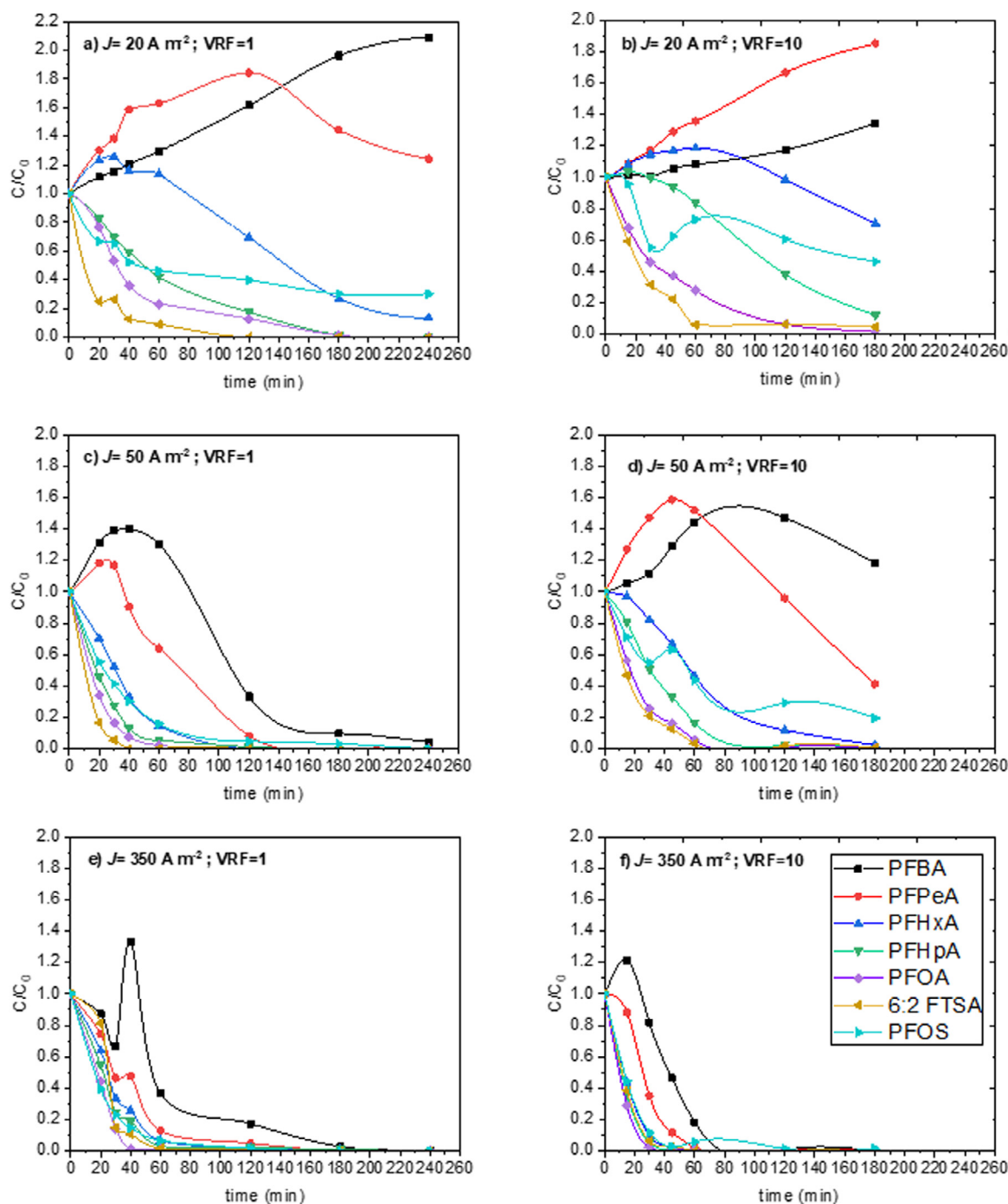
include the longest alkyl chains, continuously decreased with time at each of the tested current densities, exhibiting an exponential decay. The intermittent increase of PFOS concentration observed at 20 A m^{-2} and VRF=10 was ascribed to the experimental error. According to literature, PFOA and PFOS followed a step-by-step degradation pathway, in which a -CF$_2$- unit is lost in every degradation cycle to produce shorter-chain PFCAs, until complete mineralization [31,47,48]. Several works have reported the slower oxidation kinetics of PFOS compared to PFOA using BDD electrodes, which was attributed to the higher difficulty of the sulfonate group to initiate the direct electron transfer step [42, 45]. 6:2 FTSA degradation has been reported to start with the attack of hydroxyl radicals to one of the two unfluorinated carbons contained in the alkyl chain, being PFHxA the main initial degradation product [49]. Therefore, at the lowest applied current density (20 A m^{-2}), PFHpA, PFHxA, PFPeA and PFBA initially showed stable or increasing concentrations with time. However, at the highest current density (350 A m^{-2}), the degradation of most compounds was much faster, and only PFBA initially increased its concentration, prior to its subsequent rapid decrease. Therefore, at the highest current density (350 A m^{-2}) the kinetics of short-chain PFCAs removal were significantly faster than their generation rates.

At every applied current density, the degradation kinetics of every PFAA compound in the solution was significantly faster at VRF=1 than at VRF=10, with the exception of PFOA removal at 20 A m^{-2}. That exception could be due to the very low applied current density and the experimental uncertainty thereof. This general behaviour can be attributed to the increase of the cell potential at low VRF that is assumed to increase the anode potential, promoting faster direct electron transfer (DET) reactions at the BDD anode surface. Several studies have reported that both direct oxidation at the anode surface and electrogenerated hydroxyl radical mediated oxidation participate in the electrochemical degradation pathway of perfluorocarboxylic acids, the kinetics of the process being limited by the DET step [43,49]. The increase of the cell potential is a direct consequence of the low electrolyte concentration in the solution at constant current density conditions. For example, at J = 350 A m^{-2} and VRF=1, the average cell voltage was 43.3 ± 0.7 V, which is almost double than the cell voltage registered at VRF=10 (23.8 ± 0.6 V) at the same intensity. Empirical correlations of J_{app} vs. cell voltage (U) used in the optimization section can be found in Table S3 of the supplementary material.

With the aim of comparing different electrochemical oxidation systems, normalized first-order kinetic constants k' (normalized to electrode area and volume treated, m min^{-1}) and k'_n (current normalized,

Fig. 3. Effect of the applied current density on fractional PFAA (C/C$_0$) removal at three current density values (J = 20, 50 and 350 A m^{-2}) and two *VRF* conditions (*VRF*=1 and *VRF*=10). Lines are only for eye aid. Initial concentrations at *VRF*=1: [PFBA]$_0$ = 9.3 ± 1.3 µg L^{-1}; [PFPeA]$_0$ = 8.5 ± 1.3 µg L^{-1}; [PFHxA]$_0$ = 9.4 ± 0.9 µg L^{-1}; [PFHpA]$_0$ = 8.0 ± 1.1 µg L^{-1}; [PFOA]$_0$ = 8.5 ± 0.6 µg L^{-1}; [6:2 FTSA]$_0$ = 9.1 ± 2.2 µg L^{-1}; [PFOS]$_0$ = 6.2 ± 0.1 µg L^{-1} and 0.21 g L^{-1} Na$_2$SO$_4$ as electrolyte. Initial concentrations at *VRF*=10: [PFBA]$_0$ = 147.7 ± 1.2 µg L^{-1}; [PFPeA]$_0$ = 135.7 ± 1.7 µg L^{-1}; [PFHxA]$_0$ = 217.2 ± 4.5 µg L^{-1}; [PFHpA]$_0$ = 87.8 ± 3.2 µg L^{-1}; [PFOA]$_0$ = 111.3 ± 8.3 µg L^{-1}; [6:2 FTSA]$_0$ = 111.2 ± 12.5 µg L^{-1}; [PFOS]$_0$ = 31.5 ± 9.7 µg L^{-1} and 1.5 g L^{-1} Na$_2$SO$_4$ as electrolyte.

mal layout that resulted from the solution of the optimization problem, which includes the optimal sizing of the process, as will be discussed later. In the multistage membrane pre-concentration process, the retentate of each stage k is recycled to the previous stage *(k-1)*, except for the retentate of the first stage, which is recycled to the feed tank. The permeate is pressurized and fed to the stage *k+1*. This cascade of membrane units allows obtaining a highly purified permeate, at the same time the retentate gets concentrated in PFAAs. At the end of the pre-concentration time (t_{PC}), the remaining retentate is electrolyzed. The

ELOX system consists of a battery of *n* BDD electrochemical cells in parallel arrangement [51]. After the required electrolysis time (t_{ELOX}), the electrolyzed volume is mixed with the permeate volume from the pre-concentration process, to form the final treated volume.

A target concentration (C_{target}) is imposed at the end of the treatment train. The United States Environmental Protection Agency (USEPA) set health advisory levels for PFOS and PFOA in drinking water, individually or combined, at 0.07 µg L^{-1}. In accordance to that criterion, we evaluated a target concentration at the end of the treatment train for
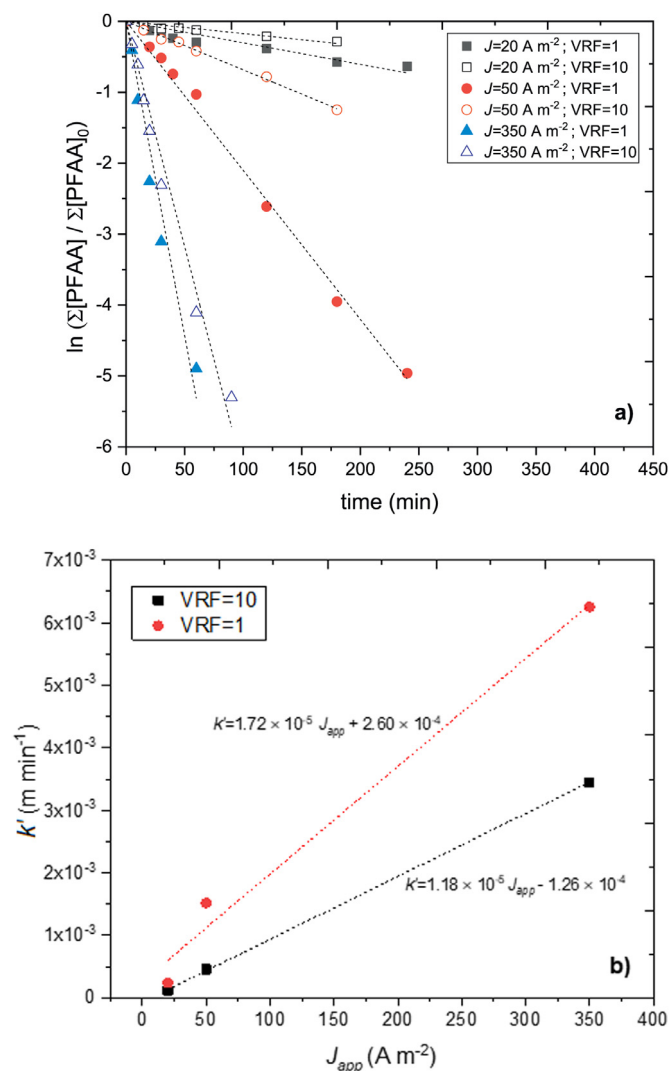
Fig. 4. a) Linearized dimensionless ΣPFAA evolution with time in electrolysis experiments at three current density values and two *VRF* conditions. Dotted lines represent the linear fitting used for determination of kinetic constants. C= Σ[PFAA], C_0= Σ[PFAA]$_0$, as given in the legend of Fig. 3. b) Linear fitting of the kinetic constant (k') of ΣPFAA removal vs. current density.

the sum of the seven PFAAs under study (PFBA, PFPeA, PFHxA, PFHpA, PFOA, PFOS and 6:2 FTSA) of 0.07 µg L^{-1}. The inlet concentration to the treatment train was set to 70 µg L^{-1} as the sum of the seven PFAAs used in this study. Therefore, a *3-log* (99.9%) $\sum_{i=1}^{7} PFAA_i$ target abatement was defined.

Information about the process modelling, equations used for the estimation of the process economics, as well as the process model input parameters can be found in the supplementary material. Additional information can be found in our previous work [34] dealing with the treatment of PFHxA in industrial process streams. Nevertheless, several novelties have been introduced to update the model to the specific needs of the treatment of groundwater impacted by AFFF: a) a new correlation for the membrane rejection of a mixture of PFAAs in the low concentration range, as described in Fig. 2 of Section 3.1; b) an overall kinetic constant has been defined to quantify the velocity of removal of the mixture of PFAAs, as shown in Fig. 4a; and iii) the effect of the applied current, at different electrolyte concentrations, on the overall kinetics of PFAA removal has been modelled, as given by the fitting equations in Fig. 4b. Also, the effect of the applied density on the cell potential has been considered (Table S3 of supplementary material). Ultimately, increasing the applied current enhanced the kinetics of PFAAs electrolysis, to unexpectedly reduce the total costs of the treatment process, as it will be shown later. Table S3 (supplementary material) summarizes the mass transfer and kinetic parameters needed to solve the optimization problem when dealing with simulated PFAAs impacted groundwater.

The integrated process was optimized based on determining the minimum total annual cost (*TC*, $ y^{-1}),

$$TC = CAPEX \frac{r(1+r)^t}{(1+r)^t - 1} + OPEX \qquad (3)$$

where *CAPEX* symbolizes the capital investment ($) and *OPEX* the annual operating expenses ($ y^{-1}). *t* is the period of time and *r* the investment rate [52], which are used to annualize the *CAPEX* term taking into account the time value of money.

The optimization problem can be mathematically formulated as,

$$\begin{aligned} min \; & TC(x) \\ s.t \quad & h(x) = 0 \\ & g(x) \geq 0 \\ & L \leq x \leq U \end{aligned} \qquad (4)$$

where *x* is the vector of decisional variables (t_{PC}, A_e, $A(k)$), *h* the vector of algebraic equations and *g* the model constraints. *L* and *U* are the lower and upper variable bounds of the decisional variables, respectively. The
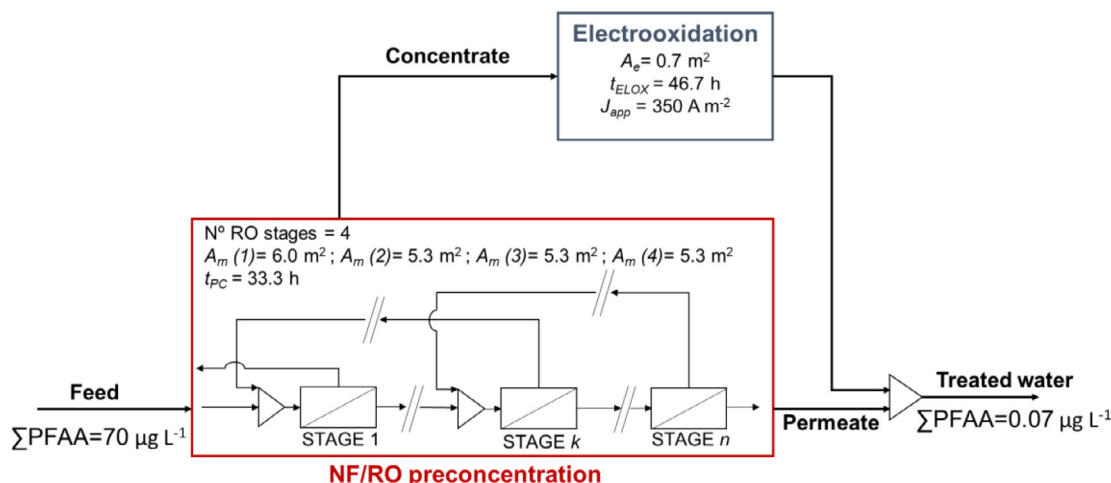

Fig. 5. Scheme of the multistage membrane pre-concentration/electrooxidation system.
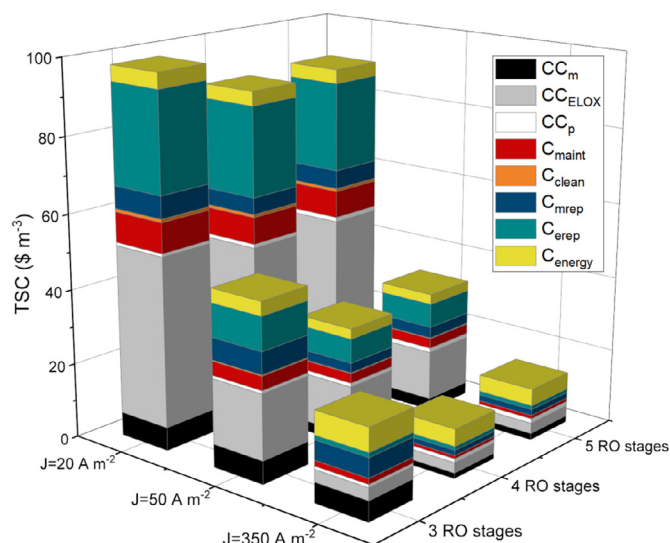
Fig. 6. Distribution of the *CAPEX (CC)* and *OPEX (C)* costs in the three to five stages membrane pre-concentration coupled to ELOX integration scenarios. Results shown at three current densities: 20, 50 and 350 A m^{-2}.

full set of equations and the strategy used for the modelling and the model input parameters can be found in the supplementary material.

We imposed a restriction to *VRF*, since reducing more than ten times the initial feed volume may cause the salts in solution to surpass their maximum solubility in water. We also restricted the membrane area per stage (A_k) in the pre-concentration system. The smallest and largest BW30 and NF90 membrane modules commercialized are 2.6 m^2 and 37 m^2, respectively. Also, the annual production (*AP*) of treated water was set to 1000 m^3 y^{-1}. The dynamic non-linear problem (NLP) describing the integrated process was implemented in the General Algebraic Modelling System (GAMS). The NLP was solved using the IPOPTH solver, an interior point optimizer for large-scale nonlinear optimization, on a 3.20 GHz Intel® Core™ i5–6500 processor.

Overall, the target concentration could be satisfactorily fulfilled with the layout formed by three, four and five preconcentration stages coupled to ELOX. The lowest total specific cost (*TSC*) was 13.1 \$ m^{-3}, that was achieved using the highest current density of 350 A m^{-2} and 4 membrane stages in the preconcentration system. Compared to the application of electrooxidation alone without previous pre-concentration, the integrated approach could save from 57.6% to 76.7% of the total costs when working at 350 A m^{-2}. In contrast, one and two stage layouts are not enough to fulfil the imposed target concentration. This is translated into a preconcentration time (t_{PC}) equal to zero, which means that the optimal solution is to eliminate the preconcentration process and directly apply the ELOX process to the fresh feed, which is equivalent to *VRF*=1. The solutions for *VRF*=1 are detailed in Table S5 of supplementary material, showing that no total cost savings are calculated in these non-optimal scenarios. Due to the extremely low PFAAs treatment requirements (0.07 µg L^{-1}), one and two stages in the preconcentration process are not enough to attain overall permeate objectives. Consequently, the PFAAs concentration at the exit of the ELOX system must be extremely low, which increases the costs related to the ELOX process (e.g. energy costs).

Fig. 6 shows the distribution of the capital and operating costs in the optimal integration scenarios, i.e., the three and four stages preconcentration layouts, using different applied current densities in the ELOX system. At low current densities ($J = 20$ A m^{-2}) the most important contribution to the total costs are the capital costs related to the investment in the ELOX reactor (CC_{ELOX}) (46.3% – 51.6%) followed by the electrode replacement costs (C_{erep}) (27.1% – 31.2%) and the membrane system capital investment (7.9% – 8.2%). The energy costs contribution

(C_{energy}) only represented a 4.3% – 7.6% of the total costs. Increasing the applied current density to $J = 350$ A m^{-2} manages to reduce the total specific costs to a minimum of 13.1 \$ m^{-3}, using 4 RO stages. In this scenario, the energy costs contribution rises to a 35.1%, as the CC_{ELOX} contribution is reduced to a 21.3%. This is because the optimal anode area is reduced from 16.2–17.7 m^2 when using $J = 20$ A m^{-2} to only 0.7–0.8 m^2 when using $J = 350$ A m^{-2}, thus decreasing CC_{ELOX} from 45355 \$ y^{-1} to only 2781 \$ y^{-1}. Therefore, the *TSC* of the integrated process are the lowest in this scenario ($J = 350$ A m^{-2}, 4 RO stages in the pre-concentration system and *VRF*=10) than in the rest of the studied scenarios. The optimal design and the value of the corresponding sizing values and optimal treatment times can be found in Fig. 5. Additionally, Table S5 of supplementary material contains the complete information (decision variables such as the membrane area per stage, electrode area, preconcentration time, as well as the electrolysis time and the value of the total costs objective function of the integrated process) of all the cases of study.

In the low current density range (20–50 A m^{-2}), the energy costs of the ELOX system of the integrated process decreases with the increase of the current density (4.1 \$ m^{-3} and 2.7 \$ m^{-3} for $J = 20$ and 50 A m^{-2}, respectively, using four membrane preconcentration stages). This is a consequence of the lower optimized anode area that is needed to meet the target concentration at higher current density using the membrane-ELOX strategy, that counterbalance the increase of the applied current density and the increase of the cell voltage, and also to the reduced electrolysis time. Therefore, the ELOX energy consumption slightly decreased from 23.2 kWh m^{-3} to 15.4 kWh m^{-3}, using J of 20 and 50 A m^{-2} respectively, and four membrane preconcentration stages. However, at very high current density ($J = 350$ A m^{-2}) the reduction of the anode area and the reduced electrolysis time is not enough to compensate the increase of the cell voltage, and the ELOX energy consumption increases to 26.0 kWh m^{-3} with the energy costs increasing to 4.6 \$ m^{-3}, using four preconcentration stages. Although previous studies on the electrochemical oxidation of PFAA found that the increase of the applied current density caused higher energy consumption [42], it should be noted that those studies did not contemplate pre-concentration strategies and the optimization of the anode area described herein. Also, in spite of the fact that we experimentally observed a linear function of the kinetic constant with the applied current density in the range of $J = 20$–350 A m^{-2} (Fig. 4b), a plateau k' value could be reached for higher J values [29]. Therefore, in that case, the energy costs of the ELOX process would inevitably rise, increasing the costs of the integrated process.

It is also worth mentioning that PFOS may be the dominant PFAA present in the influent [13,42,53]. According to Fig. 3f, working at 350 A m^{-2} all the PFAAs, including PFOS, have similar degradation kinetics; therefore, the estimation of the total costs of the integrated process would barely change. However, at low current density values (20 and 50 A m^{-2}) if PFOS is present at the highest concentrations it may slow down the overall ΣPFAA degradation kinetics. In that case, the value of the *TC* objective function would inevitably rise [34].

4. Conclusions

This work evaluates the treatment of per- and polyfluoroalkyl acids in a low concentration range (~70 µg L^{-1}, as sum of compounds), which can be found in groundwater impacted by aqueous film forming foam (AFFF) contaminated soils. It is demonstrated that in the treatment of a mixture of perfluorocarboxylic acids, perfluorooctane sulfonic acid and 6:2 fluorotelomer sulfonic acid, the optimal integration of membrane preconcentration and BDD electrochemical oxidation enables mineralization of long alkyl chain compounds (PFOA, PFOS and 6:2 FTSA) and their most recalcitrant degradation products (PFHpA, PFHxA, PFPeA and PFBA), at a much lower energy consumption and total process costs than the electrochemical treatment alone.

Due to the extremely low target concentration imposed at the end of the treatment train, it is crucial that the selectivity of the membrane

is as high as possible. In this way the highly purified permeate coming from the multistage membrane system allows to relax the required output PFAAs concentration of the ELOX reactor. This is one of the reasons why the RO membrane studied in this work was preferred over the NF membrane. Also, for treatment of low salinity groundwater, RO membranes retain ions more efficiently than NF membranes. In this way, the preconcentration approach will maximize the electrolyte conductivity, a means to achieve a substantial decrease in the voltage of the electrochemical cell, thus allowing to reduce the energy consumption of electrolysis, working at high applied current densities. In this regard, we observed that the kinetics of PFAAs electrochemical degradation was significantly enhanced at increasing applied current densities, in the range 20–350 A m^{-2}, a behaviour that was ascribed to the promotion of governing mechanism based on the direct electron transfer on the BDD electrode surface.

Finally, we demonstrate that systems engineering provides the tools for the optimal process design, using the minimization of the total cost objective function. It is concluded that a multistage membrane cascade arrangement is needed to comply with severe limits of concentration for PFOA and PFOS in the treated groundwater, using as benchmark the Health Advisory Levels established by the USEPA for drinking water. Most remarkably, the results of the current density sensitivity analysis on the total costs objective function shows that an increase of the applied current density manages to reduce the capital costs, mainly by a reduction of the anode requirements of the electrolysis system, which counterbalances the increase of the power term.

Declaration of Competing Interest

The authors declare that they have no known competing financial interests or personal relationships that could have appeared to influence the work reported in this paper.

Acknowledgements

Supplementary materials

Supplementary material associated with this article can be found, in the online version, at doi:10.1016/j.ceja.2020.100042.

References

[1] M.F. Rahman, S. Peldszus, W.B. Anderson, Behaviour and fate of perfluoroalkyl and polyfluoroalkyl substances (PFASs) in drinking water treatment: a review, Water Res. 50 (2014) 318–340, doi:10.1016/j.watres.2013.10.045.

[2] T.G. Schwanz, M. Llorca, M. Farré, D. Barceló, Perfluoroalkyl substances assessment in drinking waters from Brazil, France and Spain, Sci. Total Environ. 539 (2016) 143–152, doi:10.1016/j.scitotenv.2015.08.034.

[3] S. Castiglioni, S. Valsecchi, S. Polesello, M. Rusconi, M. Melis, M. Palmiotto, A. Manenti, E. Davoli, E. Zuccato, Sources and fate of perfluorinated compounds in the aqueous environment and in drinking water of a highly urbanized and industrialized area in Italy, J. Hazard. Mater. 282 (2015) 51–60, doi:10.1016/j.jhazmat.2014.06.007.

[4] V. Boiteux, C. Bach, V. Sagres, J. Hemard, A. Colin, C. Rosin, J.-.F. Munoz, X. Dauchy, Analysis of 29 per- and polyfluorinated compounds in water, sediment, soil and sludge by liquid chromatography-tandem mass spectrometry, Int J Environ Anal Chem 96 (2016) 705–728, doi:10.1080/03067319.2016.1196683.

[5] H. Hamid, L.Y. Li, J.R. Grace, Review of the fate and transformation of per- and polyfluoroalkyl substances (PFASs) in landfills, Environ. Pollut. 235 (2018) 74–84, doi:10.1016/j.envpol.2017.12.030.

[6] O.S. Arvaniti, E.I. Ventouri, A.S. Stasinakis, N.S. Thomaidis, Occurrence of different classes of perfluorinated compounds in Greek wastewater treatment plants and determination of their solid-water distribution coefficients, J. Hazard. Mater. 239–240 (2012) 24–31, doi:10.1016/j.jhazmat.2012.02.015.

[7] J. Bräunig, C. Baduel, A. Heffernan, A. Rotander, E. Donaldson, J.F. Mueller, Fate and redistribution of perfluoroalkyl acids through AFFF-impacted groundwater, Sci. Total Environ. 596–597 (2017) 360–368, doi:10.1016/j.scitotenv.2017.04.095.

[8] L. Ahrens, M. Bundschuh, Fate and effects of poly- and perfluoroalkyl substances in the aquatic environment: a review, Environ. Toxicol. Chem. 33 (2014) 1921–1929.

[9] W.J. Backe, T.C. Day, J.A. Field, Zwitterionic, cationic, and anionic fluorinated chemicals in aqueous film forming foam formulations and groundwater from U.S. military bases by nonaqueous large-volume injection HPLC-MS/MS, Environ. Sci. Technol. 47 (2013) 5226–5234, doi:10.1021/es3034999.

[10] E.F. Houtz, C.P. Higgins, J.A. Field, D.L. Sedlak, Persistence of perfluoroalkyl acid precursors in AFFF-impacted groundwater and soil, Environ. Sci. Technol. 47 (2013) 8187–8195, doi:10.1021/es4018877.

[11] K.C. Harding-Marjanovic, E.F. Houtz, S. Yi, J.A. Field, D.L. Sedlak, L. Alvarez-Cohen, Aerobic biotransformation of fluorotelomer thioether amido sulfonate (Lodyne) in AFFF-amended microcosms, Environ. Sci. Technol. 49 (2015) 7666–7674, doi:10.1021/acs.est.5b01219.

[12] S.R. De Solla, A.O. De Silva, R.J. Letcher, Highly elevated levels of perfluorooctane sulfonate and other perfluorinated acids found in biota and surface water downstream of an international airport, Hamilton, Ontario, Canada, Environ Int 39 (2012) 19–26, doi:10.1016/j.envint.2011.09.011.

[13] C.E. Schaefer, C. Andaya, A. Urtiaga, E.R. McKenzie, C.P. Higgins, Electrochemical treatment of perfluorooctanoic acid (PFOA) and perfluorooctane sulfonic acid (PFOS) in groundwater impacted by aqueous film forming foams (AFFFs), J. Hazard. Mater. 295 (2015) 170–175, doi:10.1016/j.jhazmat.2015.04.024.

[14] M. Filipovic, A. Woldegiorgis, K. Norström, M. Bibi, M. Lindberg, A.H. Österås, Historical usage of aqueous film forming foam: a case study of the widespread distribution of perfluoroalkyl acids from a military airport to groundwater, lakes, soils and fish, Chemosphere 129 (2015) 39–45, doi:10.1016/j.chemosphere.2014.09.005.

[15] X. Dauchy, V. Boiteux, C. Bach, A. Colin, J. Hemard, C. Rosin, J.F. Munoz, Mass flows and fate of per- and polyfluoroalkyl substances (PFASs) in the wastewater treatment plant of a fluorochemical manufacturing facility, Sci. Total Environ. 576 (2017) 549–558, doi:10.1016/j.scitotenv.2016.10.130.

[16] O.S. Arvaniti, A.S. Stasinakis, Review on the occurrence, fate and removal of perfluorinated compounds during wastewater treatment, Sci. Total Environ. 524–525 (2015) 81–92, doi:10.1016/j.scitotenv.2015.04.023.

[17] S. Woodard, J. Berry, B. Newman, Ion exchange resin for PFAS removal and pilot test comparison to GAC, Remediation 27 (2017) 19–27, doi:10.1002/rem.21515.

[18] I. Emery, D. Kempisty, B. Fain, E. Mbonimpa, Evaluation of treatment options for well water contaminated with perfluorinated alkyl substances using life cycle assessment, Int. J. Life Cycle Assess. 24 (2019) 117–128, doi:10.1007/s11367-018-1499-8.

[19] C.E. Schaefer, D. Nguyen, P. Ho, J. Im, A. Leblanc, Assessing Rapid Small-Scale Column Tests for Treatment of Perfluoroalkyl Acids by Anion Exchange Resin, Ind. Eng. Chem. Res. 58 (2019) 9701–9706, doi:10.1021/acs.iecr.9b00858.

[20] Z. Du, S. Deng, Y. Bei, Q. Huang, B. Wang, J. Huang, G. Yu, Adsorption behavior and mechanism of perfluorinated compounds on various adsorbents—A review, J. Hazard. Mater. 274 (2014) 443–454, doi:10.1016/j.jhazmat.2014.04.038.

[21] F. Li, J. Duan, S. Tian, H. Ji, Y. Zhu, Z. Wei, D. Zhao, Short-chain Per- and Polyfluoroalkyl Substances in Aquatic Systems: occurrence, Impacts and Treatment, Chem. Eng. J. 380 (2019) 122506, doi:10.1016/j.cej.2019.122506.

[22] A. Zaggia, L. Conte, L. Falletti, M. Fant, A. Chiorboli, Use of strong anion exchange resins for the removal of perfluoroalkylated substances from contaminated drinking water in batch and continuous pilot plants, Water Res. 91 (2016) 137–146, doi:10.1016/j.watres.2015.12.039.

[23] H. Lin, J. Niu, S. Liang, C. Wang, Y. Wang, F. Jin, Q. Luo, Q. Huang, Development of macroporous Magnéli phase Ti 4 O 7 ceramic materials: as an efficient anode for mineralization of poly- and perfluoroalkyl substances, Chem. Eng. J. 354 (2018) 1058–1067, doi:10.1016/j.cej.2018.07.210.

[24] T. Pancras, G. Schrauwen, T. Held, K. Baker, I. Ross, H. Slenders, Environmental Fate and Effects of poly- and perfluoroalkyl Substances (PFAS), Editor: Concawe, Brussels, Belgium, 2016.

[25] E. Steinle-Darling, M. Reinhard, Nanofiltration for trace organic contaminant removal: structure, solution, and membrane fouling effects on the rejection of perfluorochemicals, Environ. Sci. Technol. 42 (2008) 5292–5297.

[26] C.Y. Tang, Q.S. Fu, A.P. Robertson, C.S. Criddle, J.O. Leckie, Use of reverse osmosis membranes to remove Perfluorooctane Sulfonate (PFOS) from semiconductor wastewater, Environ. Sci. Technol. 40 (2006) 7343–7349, doi:10.1021/es060831q.

[27] J. Niu, Y. Li, E. Shang, Z. Xu, J. Liu, Electrochemical oxidation of perfluorinated compounds in water, Chemosphere 146 (2016) 526–538, doi:10.1016/j.chemosphere.2015.11.115.

[28] A. Urtiaga, C. Fernández-González, S. Gómez-Lavín, I. Ortiz, Kinetics of the electrochemical mineralization of perfluorooctanoic acid on ultrananocrystalline boron doped conductive diamond electrodes, Chemosphere 129 (2015) 20–26, doi:10.1016/j.chemosphere.2014.05.090.

[29] A. Urtiaga, A. Soriano, J. Carrillo-Abad, BDD anodic treatment of 6:2 fluorotelomer sulfonate (6:2 FTSA). Evaluation of operating variables and by-product formation, Chemosphere 201 (2018) 571–577, doi:10.1016/j.chemosphere.2018.03.027.

[30] C.E. Schaefer, S. Choyke, P.L. Ferguson, C. Andaya, A. Burant, A. Maizel, T.J. Strathmann, C.P. Higgins, Electrochemical transformations of perfluoroalkyl Acid (PFAA) precursors and PFAAs in groundwater impacted with aqueous film forming foams, Environ. Sci. Technol. 52 (2018) 10689–10697, doi:10.1021/acs.est.8b02726.

[31] B. Gomez-Ruiz, S. Gómez-Lavín, N. Diban, V. Boiteux, A. Colin, X. Dauchy, A. Urtiaga, Efficient electrochemical degradation of poly- and perfluoroalkyl substances (PFASs) from the effluents of an industrial wastewater treatment plant, Chem. Eng. J. 322 (2017) 196–204, doi:10.1016/j.cej.2017.04.040.

[32] P. Cañizares, R. Paz, C. Sáez, M.A. Rodrigo, Costs of the electrochemical oxidation of wastewaters: a comparison with ozonation and Fenton oxidation processes, J. Environ. Manage. 90 (2009) 410–420, doi:10.1016/j.jenvman.2007.10.010.

[33] Á. Soriano, D. Gorri, A. Urtiaga, Efficient treatment of perfluorohexanoic acid by nanofiltration followed by electrochemical degradation of the NF concentrate, Water Res. 112 (2017) 147–156, doi:10.1016/j.watres.2017.01.043.

[34] Á. Soriano, D. Gorri, L.T. Biegler, A. Urtiaga, An optimization model for the treatment of perfluorocarboxylic acids considering membrane pre-concentration and BDD electrooxidation, Water Res. 164 (2019) 114954, doi:10.1016/j.watres.2019.114954.

[35] Á. Soriano, D. Gorri, A. Urtiaga, Membrane preconcentration as an efficient tool to reduce the energy consumption of perfluorohexanoic acid electrochemical treatment, Sep Purif Technol 208 (2019) 3329–3338, doi:10.1016/j.seppur.2018.03.050.

[36] C.E. Schaefer, C. Andaya, A. Maizel, C.P. Higgins, Assessing Continued Electrochemical Treatment of Groundwater Impacted by Aqueous Film-Forming Foams, Journal of Environmental Engineering (United States) 145 (2019) 12–15, doi:10.1061/(ASCE)EE.1943-7870.0001605.

[37] W.J. Backe, T.C. Day, J.A. Field, Zwitterionic, cationic, and anionic fluorinated chemicals in aqueous film forming foam formulations and groundwater from U.S. military bases by nonaqueous large-volume injection HPLC-MS/MS, Environ. Sci. Technol. 47 (2013) 5226–5234, doi:10.1021/es3034999.

[38] Á. Soriano, D. Gorri, A. Urtiaga, Selection of High Flux Membrane for the Effective Removal of Short-Chain Perfluorocarboxylic Acids, Ind Eng Chem Res 58 (2019) acs.iecr.8b05506, doi:10.1021/acs.iecr.8b05506.

[39] J. Shen, A.I. Schäfer, Factors affecting fluoride and natural organic matter (NOM) removal from natural waters in Tanzania by nanofiltration/reverse osmosis, Sci. Total Environ. 527–528 (2015) 520–529, doi:10.1016/j.scitotenv.2015.04.037.

[40] X. Hang, X. Chen, J. Luo, W. Cao, Y. Wan, Removal and recovery of perfluorooctanoate from wastewater by nanofiltration, Sep Purif Technol 145 (2015) 120–129.

[41] T.D. Appleman, E.R.V. Dickenson, C. Bellona, C.P. Higgins, Nanofiltration and granular activated carbon treatment of perfluoroalkyl acids, J. Hazard. Mater. 260 (2013) 740–746.

[42] X. Xiao, B.A. Ulrich, B. Chen, C.P. Higgins, Sorption of Poly- and Perfluoroalkyl Substances (PFASs) relevant to aqueous film-forming foam (AFFF)-impacted groundwater by biochars and activated carbon, Environ. Sci. Technol. 51 (2017) 6342–6351, doi:10.1021/acs.est.7b00970.

[43] C.E. Schaefer, C. Andaya, A. Burant, C.W. Condee, A. Urtiaga, T.J. Strathmann, C.P. Higgins, Electrochemical treatment of perfluorooctanoic acid and perfluorooctane sulfonate: insights into mechanisms and application to groundwater treatment, Chem. Eng. J. 317 (2017) 424–432, doi:10.1016/j.cej.2017.02.107.

[44] A. Pérez-González, R. Ibáñez, P. Gómez, A.M. Urtiaga, I. Ortiz, J.A. Irabien, Nanofiltration separation of polyvalent and monovalent anions in desalination brines, J. Memb. Sci 473 (2015) 16–27, doi:10.1016/j.memsci.2014.08.045.

[45] R. Vestergren, S. Ullah, I.T. Cousins, U. Berger, A matrix effect-free method for reliable quantification of perfluoroalkyl carboxylic acids and perfluoroalkane sulfonic acids at low parts per trillion levels in dietary samples, J. Chromatogr. A 1237 (2012) 64–71, doi:10.1016/j.chroma.2012.03.023.

[46] A.I. Schäfer, I. Akanyeti, A.J.C. Semião, Micropollutant sorption to membrane polymers: a review of mechanisms for estrogens, Adv Colloid Interface Sci 164 (2011) 100–117, doi:10.1016/j.cis.2010.09.006.

[47] Q. Zhuo, S. Deng, B. Yang, J. Huang, B. Wang, T. Zhang, G. Yu, Degradation of perfluorinated compounds on a boron-doped diamond electrode, Electrochim. Acta 77 (2012) 17–22, doi:10.1016/j.electacta.2012.04.145.

[48] B. Gomez-Ruiz, S. Gómez-Lavín, N. Diban, V. Boiteux, A. Colin, X. Dauchy, A. Urtiaga, Boron doped diamond electrooxidation of 6:2 fluorotelomers and perfluorocarboxylic acids. Application to industrial wastewaters treatment, J. Electroanal. Chem. 798 (2017) 51–57, doi:10.1016/j.jelechem.2017.05.033.

[49] J. Carrillo-Abad, V. Pérez-Herranz, A. Urtiaga, Electrochemical oxidation of 6:2 fluorotelomer sulfonic acid (6:2 FTSA) on BDD: electrode characterization and mechanistic investigation, J Appl Electrochem 48 (2018) 589–596, doi:10.1007/s10800-018-1180-8.

[50] B. Gomez-Ruiz, N. Diban, A. Urtiaga, Comparison of microcrystalline and ultrananocrystalline boron doped diamond anodes: influence on perfluorooctanoic acid electrolysis, Sep Purif Technol 208 (2018) 169–177, doi:10.1016/j.seppur.2018.03.044.

[51] A. Anglada, A.M. Urtiaga, I. Ortiz, Laboratory and pilot plant scale study on the electrochemical oxidation of landfill leachate, J. Hazard. Mater. 181 (2010) 729–735, doi:10.1016/j.jhazmat.2010.05.073.

[52] L.T. Biegler, I.E. Grossmann, A.W. Westerberg, Systematic Methods of Chemical Process Design, Prentice Hall PTR, New Jersey, 1997.

[53] R.H. Anderson, G.C. Long, R.C. Porter, J.K. Anderson, Occurrence of select perfluoroalkyl substances at U.S. Air Force aqueous film-forming foam release sites other than fire-training areas: field-validation of critical fate and transport properties, Chemosphere 150 (2016) 678–685, doi:10.1016/j.chemosphere.2016.01.014.